On the Kinetic Theory of Dense Fluids. XVII. The Shear Viscosity

Bright A. Lowry, Stuart A. Rice, and Peter Gray

Citation: The Journal of Chemical Physics **40**, 3673 (1964); doi: 10.1063/1.1725072
View online: http://dx.doi.org/10.1063/1.1725072
View Table of Contents: http://scitation.aip.org/content/aip/journal/jcp/40/12?ver=pdfcov
Published by the AIP Publishing

On the Kinetic Theory of Dense Fluids. XVII. The Shear Viscosity

BRIGHT A. LOWRY,* STUART A. RICE, AND PETER GRAY†

Department of Chemistry and Institute for the Study of Metals, The University of Chicago, Chicago, Illinois

(Received 3 March 1964)

In this paper we report a theoretical study of the shear viscosity of dense fluids along with some measurements of the viscosity of liquid Ar. It is found that the theory of Rice and Allnatt leads to predictions of the temperature dependence of the shear viscosity under conditions of constant volume in good agreement with experiment. Also, the magnitudes of the predicted shear viscosity agree very well at $T=128°K$, $p=50$ atm ($\eta_{calc}=0.727\times10^{-3}$ P, $\eta_{obs}=0.835\times10^{-3}$ P) and moderately well at $T=90°K$, $p=1.3$ atm ($\eta_{calc}=1.74\times10^{-3}$ P, $\eta_{obs}=2.39\times10^{-3}$ P). The importance of obtaining accurate intermolecular pair potentials and pair correlation functions is discussed briefly.

I. INTRODUCTION

PERHAPS the most commonly measured property of a liquid is the shear viscosity. The reasons for this are easy to find: solutions of the Navier–Stokes equation for a number of simple geometries are available, and only elementary precautions are required to make accurate relative measurements in the vicinity of room temperature and atmospheric pressure. On the other hand, absolute measurements of shear viscosity or measurements at low (and high) temperatures and high pressures are extremely difficult. As a result, very few measurements of the shear viscosity of simple liquids have been reported. Since all current statistical theories of transport phenomena are restricted to the description of molecules interacting with a spherically symmetric intermolecular pair potential, it is data for the simple liquids that are required to test theory.

In this paper we present a theoretical analysis of the shear viscosity of simple liquids.[1] Previous theoretical studies of the shear viscosity may be conveniently divided into two groups. In the first group we include cell models, free volume models, and the several variants of activated state theory. As a group, these theories are characterized by the use of grossly oversimplified models, the use of adjustable parameters (activation energy) and the complete neglect of the important problem of the proper introduction of irreversibility. From the extensive experimental data available for complex liquids, it is known that at constant pressure and over a limited temperature range the viscosity is of the form $\eta=A\exp(B/T)$, with A and B constants. The activated state and cell model theories are successful in reproducing this form, but they cannot explain the relative insensitivity of the viscosity to temperature under conditions of constant volume. The free volume theory of Cohen and Turnbull[2] accounts for the constant volume temperature dependence satisfactorily (the free volume is, to first approximation, a function of density only), but again requires the use of two adjustable parameters. There can be no doubt that the theories of this group are useful and successful parameterized representations of experimental data, but the parameters cannot be quantitatively interpreted in terms of the structure of the liquid.

The second group of theories includes the various approaches based on statistical mechanics. The earliest of these is the Enskog theory of the dense rigid-sphere fluid,[3] now known to be an excellent description of rigid-sphere statistical dynamics.[4] It is interesting that Enskog suggested that the rigid-sphere theory could also be applied to real systems by replacing the pressure by the thermal pressure, $T(\partial p/\partial T)_v$. At almost the other dynamical extreme are the theories of Kirkwood and co-workers[5–7] and of Eisenschitz.[8] In each case an approach based on the Fokker–Planck equation and a Brownian motion analogy was used. (Such an approach represents a dynamical extreme in the sense that the Fokker–Planck equation is valid when momentum exchange is frequent and small relative to the mean momentum.) Kirkwood, Buff, and Green showed that the viscosity could be expressed in the form

$$\eta^{KBG}=\frac{\rho_m kT}{2\zeta}+\frac{\pi\zeta\rho^2}{15kT}\int_0^\infty R^3\frac{du(R)}{dR}\psi_2(R)g_0^{(2)}(R)dR \quad (1)$$

with ρ_m the mass density, ρ the number density, $u(R)$ the intermolecular pair potential, $g_0^{(2)}(R)$ the equilibrium pair correlation function, and ζ a friction constant arising from the total force acting on a molecule. $\psi_2(R)$ is the solution of a differential equation which will be discussed later.

* Present address: Department of Chemistry, Dartmouth College, Hanover, New Hampshire.

† Permanent address: Department of Physics, University of Newcastle-upon-Tyne, England.

[1] For a convenient review see: S. G. Brush, Theories of Liquid Viscosity, University of California, Lawrence Radiation Laboratory, Rept. No. UCRL-6400.

[2] M. H. Cohen and D. Turnbull, J. Chem. Phys. **31**, 1164 (1959).

[3] D. Enskog, Kgl. Svenska Vetenskapsakad. Handl. **63**, No. 4 (1922).

[4] B. J. Alder and T. E. Wainwright, J. Chem. Phys. **31**, 459 (1959); **33**, 1439 (1960).

[5] J. G. Kirkwood, J. Chem. Phys. **14**, 180 (1946).

[6] J. G. Kirkwood, F. P. Buff, and M. S. Green, J. Chem. Phys. **17**, 988 (1949).

[7] J. G. Kirkwood, E. K. Maun, and B. J. Alder, J. Chem. Phys. **18**, 1040 (1950).

[8] R. Eisenschitz, Proc. Phys. Soc. (London) **59**, 1030 (1947); **A62, 41** (1949); Proc. Roy. Soc. **A215**, 29 (1952).

The Enskog theory is remarkably accurate in the description of the density dependence of the high temperature viscosity of gaseous Ar.[9] For temperatures in the range 300° to 350°K (much larger than $\epsilon/k=$ 120°K with ϵ the depth of the intermolecular pair potential), the Enskog theory reproduces the viscosity of Ar up to a density of 600 amagats with an error not exceeding 10%. On the other hand, the Kirkwood theory fails at high temperatures (where large momentum transfer repulsive interactions are important), and at low temperatures leads to a predicted viscosity of liquid Ar about one-third of the observed value.[10]

Our purpose herein is to examine the predictions of the Rice–Allnatt theory.[11,12] This theory is based on separating the intermolecular pair potential into two regions: strongly repulsive and weakly attractive and repulsive. Dynamical approximations are then introduced appropriate to these two different regions and kinetic equations for the various n body distribution functions, $f^{(n)}$, are derived. The theory is designed to describe both the large momentum transfers characteristic of rigid-core encounters and the frequent small momentum transfers characteristic of quasi-Brownian motion. It has already been shown by Davis, Rice, and Meyer[13] and by Ikenberry and Rice[14] that the theory is in quantitative agreement with the observed ion mobilities and thermal conductivity in liquid Ar, Kr, Xe. For details of the theory we refer the reader to the original papers and to the recent comments by Berne, Rice, and Gray.[15] It will be shown in this paper that the Rice–Allnatt theory also gives a reasonably accurate description of the shear viscosity of simple liquids.

In addition to the theoretical analysis, we also present in this paper some preliminary experimental studies of the shear viscosity liquid Ar. Following up the early capillary flow studies of Rudenko and Schubnikow,[16] Zhdanova[17] has measured the viscosity of Ar by a dropping ball technique from 90°K to room temperature and in the density range 0.70 g cm^{-3} to 1.37 g cm^{-3}. Scott[18] has also made measurements on liquid Ar using a similar technique. The agreement between the two sets of data is poor (10% to 15%) and the reported pressure and temperature dependences are quite different. Van Itterbeck, Zink, and Pacenel[19] have measured the viscosity of Ar, but only up to the normal boiling point. Huth,[20] using an oscillating disk viscometer, studied Ne up to 44°K and Ar up to 114°K along their respective vapor–liquid coexistence lines. Although Huth's data for Ar agree with that of Rudenko and Shubnikow and Van Itterbeck, Zink and Van Pacenel, his data for N_2 disagree by 18% at 111.7°K. Since the instrument used was the same, this disagreement casts doubt on the agreement of other data sets. Finally, Boon and Thomaes[21] have made relative viscosity measurements at low pressure for Ar, Kr, and Xe and some mixtures.

In contrast to the situation sketched with respect to liquid-state data, there are excellent data available for Ar in the gas phase. Flynn, Hanks, Lemaire, and Ross[22] and Kestin[23] have made measurements from −78.5° to 100°C and up to 200 atm, and Michels, Botzen, and Schuurman[24] cover the range from 0° to 75°C at pressures up to 2000 atm. There is, in general, excellent agreement between the sets of data.

The experiments reported herein started in 1960 and were intended to provide absolute measurements of the viscosity over a wide range of temperature and pressure. In the course of our experiments, we have learned much which causes us to examine absolute viscosity measurements with great care. Although our program of measurements is not complete, we feel there is enough disagreement in the data available to warrant accompanying our theoretical analysis with some low-pressure absolute viscosity measurements on liquid Ar.

II. STATISTICAL THEORY OF THE SHEAR VISCOSITY

The viscosity of a dense fluid may be computed from the Rice–Allnatt theory using techniques similar to those employed earlier in the computation of the thermal conductivity.[14] As in that case, there are three contributions to the dissipative process. Corresponding to the flux of particles across an arbitrary reference plane, there is a net transfer of momentum which leads to a kinetic component, η_K, of the shear viscosity. Rice and Allnatt[11] have shown that η_K is given by

$$\eta_K=\frac{5kT}{8g^{(2)}(\sigma)}\frac{[1+\frac{4}{15}(\pi\rho\sigma^3)g^{(2)}(\sigma)]}{\{\Omega^{(2,2)}+[5\zeta_s/4\rho mg^{(2)}(\sigma)]\}},$$

$$\Omega^{(2,2)}=(4\pi kT/m)^{\frac{1}{2}}\sigma^2, \qquad (2)$$

where σ is a hard-core diameter and ζ_s is the friction constant arising from the autocorrelation of the soft

[9] J. Sengers, Ph.D. thesis, University of Amsterdam (1962).
[10] R. W. Zwanzig, J. G. Kirkwood, K. F. Stripp, and I. Oppenheim, J. Chem. Phys. **21**, 2050 (1953).
[11] S. A. Rice and A. R. Allnatt, J. Chem. Phys. **34**, 2144 (1961).
[12] A. R. Allnatt and S. A. Rice, J. Chem. Phys. **34**, 2156 (1961).
[13] H. T. Davis, S. A. Rice and L. Meyer, J. Chem. Phys. **37**, 947, 1521, 2470 (1962).
[14] L. Ikenberry and S. A. Rice, J. Chem. Phys. **39**, 1561 (1963).
[15] B. Berne, S. A. Rice, and P. Gray, J. Chem. Phys. **40**, 1336 (1964)
[16] N. S. Rudenko and L. Schubnikow, Physik. Z. Sowjetunion **6**, 179, 470 (1934).
[17] N. F. Zhdanova, Zh. Eksperim. i Teor. Fiz. **31**, 724 (1956); Soviet Phys.—JETP **4**, 749 (1957).
[18] R. Scott, Ph.D. thesis, Queen Mary College, University of London (1959) (unpublished).
[19] A. Van Itterbeck, H. Zink, and O. Van Pacenel, Cryogenics **2**, 210 (1962).
[20] F. Huth, Cryogenics **2**, 368 (1962); S. Forster, *ibid.* **3**, 176 (1963).
[21] J. P. Boon and G. Thomaes, Physica **29**, 208 (1963).
[22] G. P. Flynn, R. V. Hanks, N. A. Lemaire, and J. Ross, J. Chem. Phys. **38**, 154 (1963).
[23] J. Kestin and K. Pilarczyk, Trans. Am. Soc. Mech. Engrs. Paper No. 53-A-67 (1953).
[24] A. Michels, A. Botzen, and W. Schuurman, Physica **20**, 1141 (1954).

force acting on a molecule. The specific breakup of the potential into a rigid core and a softer interaction and the implications thereof are discussed in Ref. 15. For the present all that is important to note is that the strongly repulsive region of $u(R)$ is idealized as a hard-core potential.

To compute the intermolecular force contribution to the stress tensor we must obtain the pair distribution function as a function of the macroscopic gradients defining the nonequilibrium state of the fluid. Rice and Allnatt showed that the pair distribution function, $\bar{f}^{(2)}$, satisfied the equation

$$\mathfrak{D}_2\bar{f}^{(2)}(1,2)=J_1+J_2+[\zeta_s(\mathbf{R}_1)\mathfrak{A}_1+\zeta_s(\mathbf{R}_2)\mathfrak{A}_2]\bar{f}^{(2)}(1,2),$$

$$\mathfrak{D}_2\bar{f}^{(2)}=\left(\frac{\partial}{\partial t}+\frac{\mathbf{p}_1}{m}\cdot\nabla_1+\frac{\mathbf{p}_2}{m}\cdot\nabla_2+\mathbf{F}_1^{(2)}\cdot\nabla_{p1}+\mathbf{F}_2^{(2)}\cdot\nabla_{p2}\right)\bar{f}^{(2)},$$

$$\mathfrak{A}_j\bar{f}^{(2)}=\nabla_{pj}\cdot\{[(\mathbf{p}_j/m)-\mathbf{u}]\bar{f}^{(2)}+kT\nabla_{pj}\bar{f}^{(2)}\},$$

$$\mathbf{F}_j^{(2)}={}^{(2)}\langle\mathbf{F}_j^{(s)}\rangle^0+{}^{(2)}\mathbf{F}_j^{+},$$

$$J_1=\int\left[\frac{\bar{f}^{(2)}(1,2)^*\bar{f}^{(2)}(1,3)^*\bar{f}^{(2)}(2,3)^*}{f^{(1)}(1)^*f^{(1)}(2)^*\bar{f}^{(1)}(3)^*}-\frac{\bar{f}^{(2)}(1,2)\bar{f}^{(2)}(1,3)\bar{f}^{(2)}(2,3)}{\bar{f}^{(1)}(1)f^{(1)}(2)\bar{f}^{(1)}(3)}\right]\frac{p_{13}}{m}bdbd\epsilon d^3p_3,$$

$$J_2=\int\left\{\left[\frac{\bar{f}^{(2)}(1,2)^*f^{(2)}(2,3)^*g_0^{(2)}(\mathbf{R}_1,\sigma)\sigma\mathbf{k}\cdot\nabla_1\bar{f}^{(1)}(\mathbf{R}_1,\mathbf{p}_3-\Delta\mathbf{p}_3;t)}{\bar{f}^{(1)}(2)^*\bar{f}^{(1)}(3)^*}\right.\right.$$

$$\left.\left.+\left[\frac{\bar{f}^{(2)}(1,2)\bar{f}^{(2)}(2,3)g_0^{(2)}(\mathbf{R}_1,\sigma)\sigma\mathbf{k}\cdot\nabla_1\bar{f}^{(1)}(\mathbf{R}_1,\mathbf{p}_3;t)}{\bar{f}^{(1)}(2)\bar{f}^{(1)}(3)}\right]\right\}\frac{p_{13}}{m}bdbd\epsilon d^3p_3, \quad (3)$$

where ${}^{(2)}\langle\mathbf{F}_j^{(s)}\rangle^0$ is the average total soft intermolecular force on a molecule j at $\mathbf{R}$, when a pair of molecules is fixed at $\mathbf{R}_1$ and $\mathbf{R}_2$ and the average is performed in a canonical ensemble over the rest of the molecules; ${}^{(2)}\mathbf{F}_j^{+}$ is a perturbation force arising from the departure of $(f^{(N)}/f^{(3)})$ from its equilibrium value, and $\zeta_s(\mathbf{R}_1)$ is the soft friction constant for a molecule at $\mathbf{R}_1$. Of the remaining symbols in Eq. (2), m, $\mathbf{p}_j$ and $\mathbf{R}_j$ are the mass, momentum and position vector of Molecule j, b is the impact parameter and ϵ the azimuthal angle describing the hard-core binary interaction, the asterisks in J_1 and J_2 refer to the various functions following the rigid-core encounter, $\mathbf{u}$ is the mean velocity, and $\mathbf{k}$ is a unit vector lying along the line of centers when two molecules are in contact at the hard core. The solution to Eq. (3) may be shown to have the form

$$\bar{f}^{(2)}=\bar{f}_0^{(2)}\{1+\sum_{j=1}^{2}[A_j^{(1)}(\tfrac{5}{2}-W_j^2)\mathbf{W}_j\cdot\nabla_j\ln T(\mathbf{R}_j)-B_{0j}^{(1)}(\mathbf{W}_j\mathbf{W}_j-\tfrac{1}{3}W_j^2\mathbf{1}):\nabla_j\mathbf{u}(\mathbf{R}_j)+C_j\mathbf{W}_j\cdot{}^{(2)}\mathbf{G}_j^F]\}, \quad (4)$$

where

$$\bar{f}_0^{(2)}(1,2)=\frac{\rho^{(2)}(1,2)\exp(-\{[\mathbf{p}_1-m\mathbf{u}(\mathbf{R}_1)]^2/2mkT(\mathbf{R}_1)\}-\{[\mathbf{p}_2-m\mathbf{u}(\mathbf{R}_2)]^2/2mkT(\mathbf{R}_2)\})}{(2\pi mk)^3T(\mathbf{R}_1)^{\frac{3}{2}}T(\mathbf{R}_2)^{\frac{3}{2}}},$$

$$A_1^{(1)}=-\left(\frac{2kT}{m}\right)^{\frac{1}{2}}\frac{15}{4\rho g^{(2)}(1,2)}\cdot\frac{\{[1/g^{(2)}(\sigma)]+\frac{2}{5}\pi\rho\sigma^3\}}{\{8\Omega^{(2,2)}+[45\zeta_s/4\rho mg^{(2)}(1,2)g^{(2)}(\sigma)]\}}\left[1+\frac{4\Omega^{(2,2)}g^{(2)}(1,2)}{4\Omega^{(2,2)}+[45\zeta_s/4\rho mg^{(2)}(\sigma)]}\right],$$

$$C_1=(2m/kT)^{\frac{1}{2}}(1/\zeta_s),$$

$$B_{01}^{(1)}=\frac{5}{\rho g^{(2)}(1,2)}\frac{\{[1/g^{(2)}(\sigma)]+\frac{4}{15}\pi\rho\sigma^3\}}{\{8\Omega^{(2,2)}+[5\zeta_s/\rho mg^{(2)}(1,2)g^{(2)}(\sigma)]\}}\left[1+\frac{4\Omega^{(2,2)}g^{(2)}(1,2)}{4\Omega^{(2,2)}+[5\zeta_s/\rho mg^{(2)}(\sigma)]}\right],$$

$$\mathbf{W}_1=(m/2kT)^{\frac{1}{2}}[(\mathbf{p}_1/m)-\mathbf{u}],$$

$${}^{(2)}\mathbf{G}_1{}^F=\mathbf{F}_1^{(2)}+\mathbf{F}_1{}^*-kT\nabla_1\ln g^{(2)}(1,2),$$

$$={}^{(2)}\langle\mathbf{F}_1^{(s)}\rangle^0+{}^{(2)}\mathbf{F}_1{}^+-{}^{(1)}\langle\mathbf{F}_1^{(s)}\rangle^0-{}^{(1)}\mathbf{F}_1{}^+-kT\nabla_1\ln g^{(2)}(1,2). \quad (5)$$

The intermolecular force contribution to the viscosity is conveniently subdivided into two contributions corresponding to the two regions of the intermolecular pair potential. The computation of the contribution arising from the transfer of momentum which occurs during a rigid-core encounter is similar in form to that arising in the pure rigid-sphere fluid. Taking account of the discontinuous character of a rigid-sphere potential, we find by

application of techniques used previously[14] the contribution

$$\eta_V(\sigma)=\eta_V^{(1)}(\sigma)+\eta_V^{(2)}(\sigma)+\eta_V^{(3)}(\sigma),$$

$$\eta_V^{(1)}(\sigma)=\frac{5kT}{8g^{(2)}(\sigma)}\left(\frac{2\pi\rho\sigma^3}{15}\right)\left[1+\frac{4\pi\rho\sigma^3}{15}g^{(2)}(\sigma)\right]\mathbf{D},$$

$$\mathbf{D}=\left[\Omega^{(2,2)}+\frac{5\zeta_s}{8\rho m[g^{(2)}(\sigma)]^2}\right]^{-1}\left[1+\frac{4\Omega^{(2,2)}g^{(2)}(\sigma)}{4\Omega^{(2,2)}+[5\zeta_s/\rho m g^{(2)}(\sigma)]}\right],$$

$$\eta_V^{(2)}(\sigma)=\frac{8\pi}{15}\frac{\rho^2\sigma^6 g^{(2)}(\sigma)}{\Omega^{(2,2)}}kT;\qquad \eta_V^{(3)}(\sigma)=-\frac{37}{70}\left(\frac{2\pi\rho\sigma^3}{15}\right)\rho g^{(2)}(\sigma)\zeta_s\psi_2(\sigma). \tag{6}$$

The reader will note that in addition to the modified Enskog terms, $\eta_V^{(1)}(\sigma)$ and $\eta_V^{(2)}(\sigma)$, there is a contribution to the shear viscosity arising from the distortion of the radial distribution function away from spherical symmetry. The magnitude of the distortion at $R_{12}=\sigma$ is determined by $\psi_2(\sigma)$, the evaluation of which is discussed next. However, before discussing the calculation of the distortion to $g^{(2)}$ it is important to remark that $\eta_V^{(3)}(\sigma)$ is linear in ζ_s and therefore vanishes for the fluid of rigid spheres. In a sense, this term represents a *cross effect* between the rigid-core potential and the soft potential, since the distortion is determined by the soft potential. The contribution $\eta_V^{(3)}(\sigma)$ is unique to a theory which includes both strongly repulsive forces and soft forces, and does not appear explicitly in either the rigid-core limit or the Brownian motion limit.

The contribution to the shear viscosity from the region $R>\sigma$ arises from the distortion of the pair correlation function in the flow of the liquid. To calculate this component of η we use the arguments introduced by Kirkwood, Buff, and Green[6] and start from the exact relation between the stress tensor $\mathfrak{d}$ and the intermolecular potential. This is[25]

$$\mathfrak{d}_V=\tfrac{1}{2}\sum_j\sum_k \times\int_\tau^{-1}\int \mathbf{R}_{jk}\nabla_{jk}u\delta(\mathbf{R}_j-\mathbf{R}_2)\delta(\mathbf{R}_k-\mathbf{R})f^{(N)}ds d\Gamma_N d^3R_{12} \tag{7}$$

which is readily reduced to

$$\mathfrak{d}_V=\tfrac{1}{2}N^2\int \mathbf{R}_{12}\nabla_{12}u\tilde{f}^{(2)}(1,2)d^3R_{12}d^3p_1d^3p_2. \tag{8}$$

To calculate the deformation of $g^{(2)}(R)$ due to the flow field we digress and examine the conservation of number density and momentum in phase space under conditions wherein a pair of molecules is always separated by distances greater than σ. For this region of phase space, Eq. (3) reduces to the Fokker–Planck equation. We define the current density in pair space by

$$\mathbf{j}_1^{(2)}=\int\frac{\mathbf{p}_1}{m}\tilde{f}^{(2)}(1,2)d^3p_1d^3p_2. \tag{9}$$

[25] J. H. Irving and J. G. Kirkwood, J. Chem. Phys. **18**, 817 (1950).

Now multiply Eq. (3) (with $J_1=J_2=0$) by 1 and $\mathbf{p}$ and integrate over d^3p_1 and d^3p_2 to find

$$\begin{aligned}
&(\partial\rho^{(2)}/\partial t)+\nabla_1\cdot\mathbf{j}_1^{(2)}+\nabla_2\cdot\mathbf{j}_2^{(2)}=0,\\
&m(\partial\mathbf{j}_1^{(2)}/\partial t)=-kT\nabla_1\rho^{(2)}+\mathbf{F}_1^{(2)}\rho^{(2)}\\
&\qquad\qquad -\zeta_s(\mathbf{R}_1)[\mathbf{j}_1^{(2)}-\mathbf{u}(\mathbf{R}_1)\rho^{(2)}],\\
&m(\partial\mathbf{j}_2^{(2)}/\partial t)=-kT\nabla_2\rho^{(2)}+\mathbf{F}_2^{(2)}\rho^{(2)}\\
&\qquad\qquad -\zeta_s(\mathbf{R}_2)[\mathbf{j}_2^{(2)}-\mathbf{u}(\mathbf{R}_2)\rho^{(2)}],\\
&m[\partial(\rho\mathbf{u})/\partial t]=-kT\nabla_1\rho(\mathbf{R}_1)+\mathbf{F}_1^{(1)}\rho(\mathbf{R}_1),\\
&[\partial\rho(\mathbf{R}_1)/\partial t]+\nabla_1\cdot(\rho\mathbf{u}(\mathbf{R}_1))=0,
\end{aligned} \tag{10}$$

after neglect of nonlinear terms in $\mathbf{u}$. To proceed further we must evaluate the forces $\mathbf{F}_2^{(2)},\cdots$, in terms of known quantities. If the surroundings of a pair of molecules is in local equilibrium, the perturbation contribution to $\mathbf{F}_2^{(2)},\cdots$, vanishes. We then have

$$\mathbf{F}_i^{(2)}-\mathbf{F}_i^{(1)}=kT\nabla_i\ln g_0^{(2)};\qquad R>\sigma. \tag{11}$$

Introduction of the definition of $g^{(2)}(R)$ in terms of $\rho(\mathbf{R}_1)\rho(\mathbf{R}_2)$ into (10), the elimination of $(\partial\rho/\partial t)$ by use of the conservation equations, and the neglect of inertial terms leads to the equations

$$\begin{aligned}
&\nabla_{12}\cdot\{\nabla_{12}g^{(2)}-(\nabla_{12}\ln g_0^{(2)})g^{(2)}\}\\
&\qquad -\frac{\zeta_s}{2kT}\frac{\partial g^{(2)}}{\partial t}=\frac{\zeta_s}{2kT}\mathbf{R}_{12}\cdot\boldsymbol{\varepsilon}\cdot\nabla_{12}g^{(2)},\\
&\mathbf{j}_{12}^{(2)}=-(2kT/\zeta_s)\{\nabla_{12}g^{(2)}-(\nabla_{12}\ln g_0^{(2)})g^{(2)}\},\\
&\rho(\mathbf{R}_1)\rho(\mathbf{R}_2)\mathbf{j}_{12}^{(2)}=[\mathbf{j}_2^{(2)}-\rho^{(2)}\mathbf{u}(\mathbf{R}_2)]\\
&\qquad -[\mathbf{j}_1^{(2)}-\rho^{(2)}\mathbf{u}(\mathbf{R}_1)],
\end{aligned} \tag{12}$$

and we have used the expansion

$$\begin{aligned}
&\mathbf{u}(\mathbf{R}_2)=\mathbf{u}(\mathbf{R}_1)+\mathbf{R}_{12}\cdot\nabla_{12}\mathbf{u}\\
&\boldsymbol{\varepsilon}=\mathrm{Sym}\nabla\mathbf{u}=\tfrac{1}{2}(\nabla\mathbf{u}+(\nabla\mathbf{u})^\dagger).
\end{aligned} \tag{13}$$

Note that $\mathbf{j}_{12}^{(2)}$ is the excess pair flux in relative ($\mathbf{R}_{12}$) pair space. Clearly, $\mathbf{j}_{12}^{(2)}$ must vanish as $R_{12}\to\infty$, and must also be conditioned by the absence of sources or sinks in the pair density distribution.

For the steady state, $(\partial g^{(2)}/\partial t)=0$, and we may use the expansion

$$\begin{aligned}\mathbf{R}_{12}\cdot\boldsymbol{\varepsilon}\cdot\mathbf{R}_{12}/R_{12}^2=&\tfrac{1}{3}\varepsilon_{xy}P_2^{(2)}(\cos\vartheta)\,\sin 2\varphi\\&+\tfrac{2}{3}\varepsilon_{xz}P_2^{(1)}(\cos\vartheta)\,\cos\varphi\\&+\tfrac{2}{3}\varepsilon_{yz}P_2^{(1)}(\cos\vartheta)\,\sin\varphi\\&+(\varepsilon_{zz}-\tfrac{1}{3}\nabla\cdot\mathbf{u})\,P_2^{(0)}(\cos\vartheta)\\&+\tfrac{1}{6}(\varepsilon_{xx}-\varepsilon_{yy})\,P_2^{(2)}(\cos\vartheta)\,\cos 2\varphi\\&+\tfrac{1}{3}\nabla\cdot\mathbf{u}P_0^{(0)}(\cos\vartheta),\end{aligned}\tag{14}$$

where the $P_n^{(m)}$ are associated Legendre polynomials. With the expansion (14), we may write for the pair correlation function

$$g^{(2)}=g_0^{(2)}\left[1+\frac{\zeta_s}{2kT}\left(\frac{\mathbf{R}_{12}\cdot\boldsymbol{\varepsilon}\cdot\mathbf{R}_{12}}{R_{12}^2}-\tfrac{1}{3}\nabla\cdot\mathbf{u}\right)\psi_2(R_{12})+\frac{\zeta_s}{6kT}(\nabla\cdot\mathbf{u})\psi_0(R_{12})\right],\tag{15}$$

where $\psi_2(R_{12})$ is the coefficient of Legendre polynomials of order two, arising from the shear components of the rate of strain, and $\psi_0(R_{12})$ is the coefficient of the polynomial of order zero. Introduction of (15) into (12) and linearization with respect to the components of the rate of strain leads to an ordinary differential equation determining ψ_2. This equation is

$$\frac{d}{dR_{12}}\left(R_{12}^2g_0^{(2)}\frac{d\psi_2}{dR_{12}}\right)-6g_0^{(2)}\psi_2=R_{12}^3\frac{dg_0^{(2)}}{dR_{12}}.\tag{16}$$

To determine the boundary conditions we examine the excess flux $\mathbf{j}_{12}^{(2)}$ after substitution of (15) into (12):

$$\mathbf{j}_{12}^{(2)}=-g_0^{(2)}\{\nabla_{12}[(\mathbf{R}_{12}\cdot\boldsymbol{\varepsilon}\cdot\mathbf{R}_{12}/R_{12}^2)-\tfrac{1}{3}\nabla\cdot\mathbf{u}]\psi_2+\tfrac{1}{3}(\nabla\cdot\mathbf{u})\psi_0\}.\tag{17}$$

The function ψ_0 is required for the theory of bulk viscosity and will not be needed herein. The requirement that $\mathbf{j}_{12}^{(2)}=0$ when $R_{12}\to\infty$ leads to

$$\lim_{R_{12}\to\infty}\psi_2(R_{12})=0\tag{18}$$

and the requirement that the normal component of $\mathbf{j}_{12}$ vanishes at the surface of the rigid core leads to

$$\lim_{R_{12}\to\sigma}R_{12}^2g_0^{(2)}(d\psi_2/dR_{12})=0.\tag{19}$$

Of course, $\psi_2(R_{12})$ and its derivative must be continuous everywhere in the range $\sigma<R_{12}<\infty$. Finally, the substitution of (15) into (8) leads to the intermolecular force contribution to the shear viscosity:

$$\eta_V(R_{12}>\sigma)=\frac{\pi\zeta_s\rho^2}{15kT}\int_\sigma^\infty R_{12}^3\frac{du}{dR_{12}}g_0^{(2)}(R_{12})\psi_2(R_{12})\,dR_{12}.\tag{20}$$

In deriving Eq. (20), the term ${}^{(2)}\mathbf{G}_1^F$ need not be considered since it leads to a higher order contribution to the stress tensor which is not linear in $\nabla\mathbf{u}$. Note the similarity of this integral form to that determining the pressure in terms of $g^{(2)}(R)$. We may anticipate that (20) will be as sensitive to the relative positions of the minimum of u and the first maximum of $g^{(2)}(R)$ as is the pressure integral. The reader should also note the similarity of (20) to the second term of Eq. (1). The difference between these is in the lower limit of integration and the domain over which ψ_2 is defined, as well as the substitution of ζ_s for ζ. Despite the apparently small changes, the effect of excluding the strongly repulsive forces and treating them separately markedly alters the predicted viscosity.

III. SOME NUMERICAL CALCULATIONS

We have calculated theoretical values for the shear viscosity of argon at 128°K and 50 atm, 133.5°K and 100 atm, 185.5°K and 500 atm and 90°K and 1.3 atm. These are the same points for which Ikenberry and Rice[14] made theoretical calculations of the thermal conductivity of argon. The first three points are along a line of constant density ($\rho_m=1.12$ g/cm^3) and were chosen because it was felt that the theoretical radial distribution function was better in this region than in the normal liquid phase. The 90°K point was chosen because other theoretical calculations of the shear viscosity and thermal conductivity have been made for this temperature and pressure. The contributions η_K and $\eta_V(R_{12}=\sigma)$ were calculated directly from the analytic expressions (2) and (6), while $\eta_V(R_{12}>\sigma)$ was obtained by the numerical integration of Eq. (20). In this latter calculation we followed closely the method of Zwanzig *et al.*[10]

In order to calculate $\psi_2(R_{12})$, we transform the differential Eq. (16) and its boundary condition to the corresponding integral equation ($x=R_{12}/\sigma$):

$$-\psi_2(x)=6\int_x^\infty\frac{1}{s^2g_0^{(2)}(s)}\int_1^s g_0^{(2)}(t)\psi_2(t)\,dt\,ds+\int_x^\infty\frac{1}{s^2g_0^{(2)}(s)}\int_1^s t^3\frac{dg_0^{(2)}}{dt}\,dt\,ds,\tag{21}$$

where we have assumed that the hard-sphere cutoff in the potential is at $R_{12}=\sigma(x=1)$. It is convenient to make the following definitions:

$$A(x)=\int_x^\infty\frac{ds}{s^2g_0^{(2)}(s)},$$

$$B(x)=\int_x^\infty s^2[g_0^{(2)}(s)-1]\,ds,$$

$$C(x)=\int_x^\infty s^2[g_0^{(2)}(s)-1]A(s)\,ds,$$

$$D(x)=\int_x^\infty\left[\frac{s}{g_0^{(2)}(s)}-s\right]ds.$$

TABLE I. Numerical results of theoretical calculations for the shear viscosity of argon.[a]

	50 atm 128°K	100 atm 133.5°K	500 atm 185.5°K	1.3 atm 90°K
P	4.39	4.44	5.16	3.96
η(calc)	0.692	0.701	0.865 0.745[b]	1.207
C	0.9819	0.9827	0.9887	0.9705
Corrected η(calc)	0.727	0.730	0.874 0.753[b]	1.74
$\eta_v(R>\sigma)$	0.1844	0.1898	0.1114	0.9258
Corrected $\eta_v(R>\sigma)$	0.2215	0.2228	0.1206	1.256

[a] Viscosity is expressed in units of millipoise.
[b] $g^{(2)}(\sigma)=1$.

The integrals with limits of 1 to s are now changed to integrals from 1 to ∞ minus the integrals from s to ∞ and the terms involving $dg_0^{(2)}(u)/du$ integrated by parts in the following manner:

$$\int_s^\infty t^3\frac{dg_0^{(2)}}{dt}dt=\{t^3[g_0^{(2)}(t)-1]\}_s^\infty-3\int_s^\infty t^2[g_0^{(2)}(t)-1]dt.$$

We also make use of the identity

$$\int_x^\infty A(s)\int_s^\infty B(t)dtds$$
$$=\int_x^\infty A(s)ds\int_x^\infty B(s)ds-\int_x^\infty B(s)\int_s^\infty A(t)dtds.$$
$$\lim_{x\to\infty}A(x)=0,$$
$$\lim_{x\to\infty}B(x)=0.$$

After these manipulations, Eq. (21) reduces to

$$\psi_2(x)=D(x)-3A(x)B(x)+3C(x)$$
$$+6A(x)\int_x^\infty g_0^{(2)}(s)\psi_2(s)ds$$
$$-6\int_x^\infty A(s)g_0^{(2)}(s)\psi_2(s)ds. \quad (22)$$

To evaluate these integrals, it is assumed that

$$\psi_2(x)=P/x^3; \qquad x\geq 7.$$

P is a constant which must be determined. The integrals of Eq. (22) were then evaluated for x less than 7 by the trapezoidal rule with a mesh of 0.005. As in earlier work, the radial distribution functions of Kirkwood, Lewinson, and Alder[26] were used; it was assumed that these were unity for x greater than 7. This choice of radial distribution function is consistent with the potential

$$u(R)=\infty; \qquad R<\sigma \qquad (x<1),$$
$$u(R)=4\epsilon(x^{-12}-x^{-6}); \qquad R\geq\sigma \qquad (x\geq 1),$$

with ϵ the depth and σ the distance at which $u=0$. This potential, which we have used previously, will be employed throughout the remainder of this paper.

Since A, B, C, and D are known functions of x, it is clear that Eq. (22) will give a family of functions $\psi_2(x, P)$. The correct value of P will be that for which $\psi_2(x, P)$ satisfies the boundary condition at $x=1$. If the differential equation for $\psi_2(x)$ is integrated once, it is found that

$$x^2g_0^{(2)}(x)\frac{d\psi_2}{dx}=6\int_1^x g_0^{(2)}(s)\psi_2(s)ds+\int_1^x s^3\frac{dg_0^{(2)}(s)}{ds}ds \quad (23)$$

and the boundary conditions required that (23) be zero in the limit as x approaches infinity

$$\int_1^\infty g_0^{(2)}(s)\psi_2(s)ds$$
$$=-\tfrac{1}{6}(\{s^3[g_0^{(2)}(s)-1]\}_1^\infty-3\int_1^\infty s^2[g_0^{(2)}(s)-1]ds)$$
$$=\tfrac{1}{6}[g_0^{(2)}(1)-1]+\tfrac{1}{2}B(1). \quad (24)$$

The right-hand side of this equation is known. Since every value of $\psi_2(x, P)$ is linear in P, the left-hand side of the equation is linear in P. This then gives us a method of finding the value of P which will satisfy the boundary conditions. The procedure is as follows: Two values of P are chosen and the corresponding $\psi_2(x, P)$ computed and used to evaluate the integral on the left-hand side of the equation. The computed values are then compared with the value on the right-hand side and a linear interpolation leads to the correct value of P.

TABLE II. Sensitivity of the calculated shear viscosity[a] to the core size, σ.

p	T	$\eta_K\times10^4$	$\eta_V(\sigma)\times10^4$	$\eta_V(R>\sigma)\times10^4$	$\eta\times10^3$ (calc)
		$\sigma=3.418\times10^{-8}$ cm			
50	128	0.590	4.47	2.21	0.727
100	133.5	0.586	4.48	2.23	0.730
500	185.5	0.951	6.58	1.20	0.874
			5.37[b]		0.753[b]
1.3	90	0.308	4.47	12.56	1.74
		$\sigma=3.349\times10^{-8}$ cm			
50	128	0.576	4.10	2.03	0.671
100	133.5	0.573	4.11	2.06	0.674
500	185.5	0.923	5.77	1.13	0.782
			4.93[b]		0.698[b]
1.3	90	0.302	4.07	11.68	1.65

[a] Viscosity is expressed in units of poise.
[b] $g^{(2)}(\sigma)=1$.

[26] J. G. Kirkwood, V. A. Lewinson and B. J. Alder, J. Chem. Phys. 20, 929 (1952).

The numerical calculations were made using an IBM 7094. The data from Kirkwood, Lewinson, and Alder were introduced along with the appropriate temperatures. The machine computed and stored in memory $A(x)$, $B(x)$, $C(x)$, $D(x)$, and $g(x)$ at intervals of 0.005 for $1\leq x\leq 7$; $\psi_2(x, P)$ was evaluated for $P=1$ and $P=2$. These functions were used to compute the integral of Eq. (24), the correct value of P, $\psi_2(x, P)$ was recomputed and then, if the left-hand side of Eq. (24) agreed with the right-hand side to within 0.1%, the machine used these $\psi_2(x)$ functions to evaluate the integral of Eq. (22). Again, we used the trapezoidal rule and a mesh of 0.005.

The values of η_K, $\eta_V(\sigma)$, P, $\eta_V(R>\sigma)$, and η are given in Tables I and II.

A closer examination of the numerical integration is discouraging. The functions $g_0^{(2)}(x)$, $\psi_2(x)$, and $du(x)/dx$ all vary widely and the latter two can be either positive or negative. The negative parts of the integral tend to cancel the positive parts so that the value is very sensitive to the relative shape and positions of $u(x)$, $g_0^{(2)}(x)$, and $\psi_2(x)$. A similar case of numerical discouragement is found in the computation of the equation of state. Using the modified Lennard-Jones potential

$$\frac{p}{\rho kT}=1+2\pi\rho\sigma^3 g_0^{(2)}(\sigma)-\frac{8\pi\rho\sigma^3\epsilon}{3kT}\int_1^\infty x^3\frac{du}{dx}g_0^{(2)}(x)dx, \quad (25)$$

which is also sensitive to the shape and relative positions of $u(x)$ and $g(x)$. Using the temperatures and distribution functions cited, Eq. (25) predicts large negative values for the pressure. However, one need only change the relative positions of $du(x)/dx$ and $g_0^{(2)}(x)$ by about 2% to obtain the correct pressure. By replacing $du(x)/dx$ by $du(cx)/dcx$, where c is a number close to unity, such a relative shift is easily introduced into Eqs. (20) and (25).

Since the pressure integral is similar in form to the viscosity integral, it can be argued that partial compensation for the lack of accurate knowledge of $g_0^{(2)}(x)$ and $u(x)$ is achieved by using Eq. (25) to obtain a value for c and then using this value of c in the viscosity equation. The results of this computation are displayed in Table I. It should be noted that the changes in potential required are within the experimental uncertainty in $u(R)$.

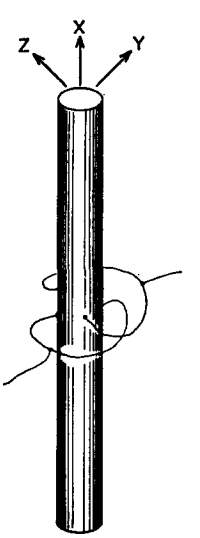

FIG. 1. The X-cut quartz crystal.

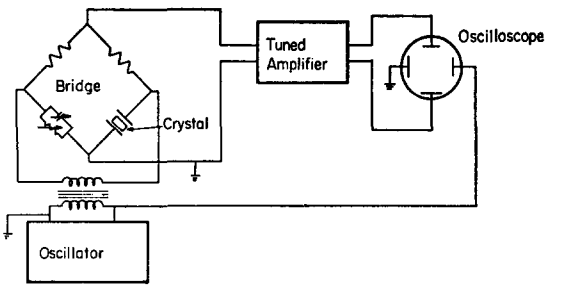

FIG. 2. Block diagram of the electrical circuitry.

There is at least one other large source of uncertainty in our calculations: It is difficult to estimate how accurately σ is known since there is more than 5% variation in the literature values for σ. The uncertainty in σ is particularly unfortunate because fifth and sixth powers of σ appear in our equations. The effect of varying σ is displayed in Table II.

We defer comments on the calculations described in this section until Sec. V.

IV. EXPERIMENTAL DETAILS AND PRELIMINARY RESULTS

The viscosity of fluid Ar was measured by studying the damping of a torsionally oscillating quartz crystal. This method has been described in some detail by Mason[27] and Welber.[28]

The crystal is illustrated in Fig. 1. It was cut in the shape of a cylinder, 6 cm long and 6 mm in diameter, the axis of the cylinder being along the x axis of the crystal. Four gold electrodes were deposited by vapor condensation along the length of the crystal, and the opposite pairs connected together. The center lines of the electrodes make 45° angles with the y axis. The resonant frequency of the crystal used in our measurements was 32.6 kc/sec

It may be shown that, for a torsionally oscillating piezoelectric crystal,[27,28]

$$\eta\rho_m=(\nu_0/\pi)[M(\Delta-\Delta_0)/\mathcal{S}]^2, \quad (26a)$$

$$R-R_0=\frac{r_0^3+r_0^4/l}{4\pi\nu_0(\nu_A-\nu_0)C_0 I}(\pi\nu_0\eta\rho_m)^{\frac{1}{2}}, \quad (26b)$$

where R is the electrical resistance at resonance in the fluid, R_0 is the electrical resistance in vacuum, ν_0 is the

[27] W. P. Mason, Trans. Am. Soc. Mech. Engrs. **69**, 359 (1947). W. P. Mason, *Piezoelectric Crystals and Their Applications to Ultrasonics* (D. Van Nostrand Company, Princeton, New Jersey 1950).

[28] B. Welber, Phys. Rev. **119**, 1816 (1960).

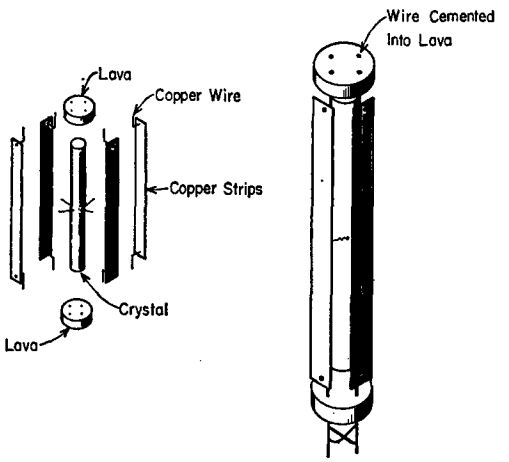

FIG. 3. The crystal holder.

resonant frequency in vacuum and ν_A is the anti-resonant frequency, r_0 and l are the radius and length of the crystal, I and C_0 are the moment of inertia per unit length and static capacitance of the crystal, M and S are the mass and surface area of the crystal, and Δ and Δ_0 are the logarithmic decrements in the fluid and in vacuum.

Either of Eqs. (26) may be used to compute η from experimental data, but it is our opinion that for quartz crystals (26a) is superior to (26b). The use of (26b) requires a knowledge of $\nu_A-\nu_0$, and for our particular crystal this was about 1.5 cps, a number difficult to measure accurately at 32 kc/sec.

A schematic diagram of the electrical circuit used is given in Fig. 2. The oscillator is a General Radio 713-B beat frequency oscillator, and the ac bridge is a General Radio 716-C capacitance bridge suitably modified by the addition of a set of calibrated resistors. Frequency was measured with an accuracy of ± 0.1 cps with a Hewlett-Packard 523 DR electronic counter. To amplify the bridge signal, we used a Keithley Model 102 isolation amplifier plus a home-made tuned pre-amplifier.

Two types of resistors were used in the balancing arm of the bridge circuit. Below $10^4\ \Omega$ a General Radio Type 1432N decade resistance box was employed, while above $10^4\ \Omega$ highly stable molded metal film resistors (International Resistance Company Type MEA-TO) were used. These were calibrated with a Jones bridge. With this arrangement it was possible to measure resistances up to 300 kΩ in steps of 0.1 Ω.

The crystal holder is shown in Fig. 3. The wires from the crystal are soldered to four copper strips which are held in place by lava plugs at either end. The only supports for the crystal are in the lead-in wires which

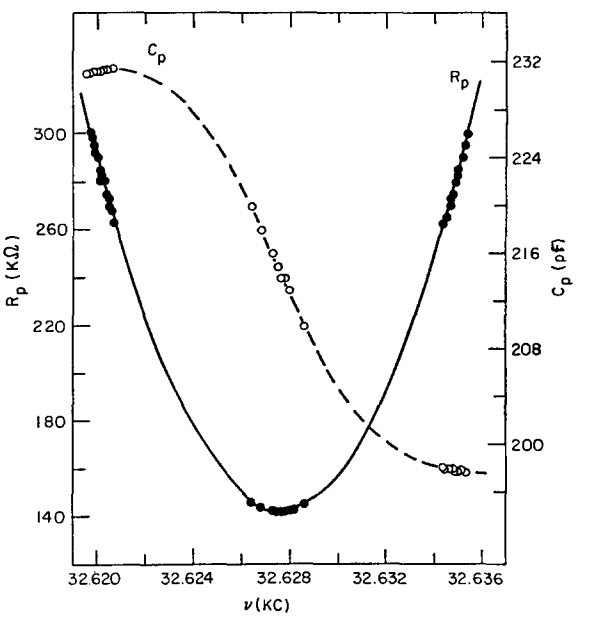

FIG. 5. A typical resonance curve.

are soldered to the crystal at the nodal point in the center. The crystal was ground by the Crystal Optics Company of Chicago, Illinois, and the electrodes attached by the James Knights Company of Sandwich, Illinois. Measurements using a traveling microscope indicate that the crystal is round to 0.1 mm. An optical finish was put on the crystal surface.

The pressure cell (Fig. 4) consists of a stainless steel body which has had a copper jacket sweated on to minimize temperature gradients. The temperature was measured with a 30-gauge copper-constantan thermocouple (not shown), which was located in the fluid, a few millimeters below the bottom of the crystal. The thermocouple wires and the wires to the crystal were brought out through a slightly modified Conax thermocouple assembly (TG-14B4). A compressed Lavite packing made the pressure seal around the wires. The gases were introduced through a high pressure tube at

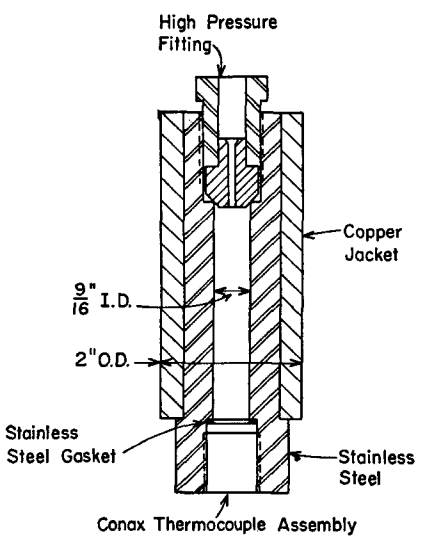

FIG. 4. The pressure cell.

the top of the cell. The cell was built by Autoclave Engineers and has a pressure rating of 10 000 psi.

The thermocouple emf was measured on a Leeds & Northrup K-3 potentiometer, and the temperature was recorded to the nearest 0.1°K. The thermocouple wire itself was obtained from a roll that was very carefully calibrated by Ikenberry and Rice.

Liquid nitrogen was used as the coolant. The pressure cell was suspended in a tall Dewar, a few inches above the surface of the nitrogen. A heat leak consisting of a copper rod $\frac{1}{2}$ in. in diameter and 8 in. long was screwed into the bottom of the cell and extended into the liquid nitrogen. The rod was shielded from the coolant by a copper cup soldered to the bottom of the rod, so that only the end of the rod was exposed. If the rod were not shielded, the amount of heat flowing down the rod would depend on the level of the liquid nitrogen. This arrangement would cool the bomb down to about 92°K.

The cell temperature was controlled automatically. A thermometer which consisted of 40 gauge copper wire wrapped around a copper spool was screwed into the copper jacket of the pressure cell. This thermometer was made from one arm of a 60-cycle ac resistance bridge. The output of this bridge controlled the solid-state equivalent of a thyratron tube, which in turn controlled the amount of current supplied to the heating coil. The heating coil was nichrome wire wrapped around the outside of the bomb.

The pressure was generated by alternately freezing and vaporizing the substance being studied, in a pair of 1cc cells. Pressure was measured on two calibrated (0.1%) Heise pressure gauges to an accuracy of 1% or better.

The electrical resistance of the crystal was measured to a precision of 0.1% in the high-density fluid and 1% in the low-density fluid. Since the decrement Δ is proportional to the resistance of the crystal, Eq. (26a) may then be used to evaluate the product $\eta\rho_m$.

There remains to be discussed only the method used to measure the decrement, Δ, and the necessary corrections to our measurements. If W_0^d is the energy dissipated per cycle due to the internal friction of the crystal, then the Q for the system is given by

$$Q=2\pi[W^\nu/(W_{\text{fluid}}{}^d+W_0{}^d)] \tag{27}$$

from which the logarithmic decrement becomes

$$\Delta=\frac{\pi/Q}{(1-4/Q^2)^{\frac{1}{2}}}\approx\frac{\pi}{Q}, \tag{28a}$$

$$\Delta=(W_{\text{fluid}}{}^d+W_0{}^d)/2W^\nu=(W_{\text{fluid}}{}^d/2W_0{}^\nu)+\Delta_0. \tag{28b}$$

TABLE III. Data used to compute the longitudinal loading correction.

Substance	T (°C)	R ($k\Omega$)	$\nu\times10^{-3}$ cps	ρ_m (g cm^{-3})	$\eta\rho_m\times10^3$
Benzene	26.0	104.6	32.61	0.8724	5.175

TABLE IV. Test of measurements by comparison with NBS standard oil.

Substance	T (°C)	R ($k\Omega$)	$\nu\times10^{-3}$ cps	ρ_m (g cm^{-3})	$\eta\rho_m\times10^3$ (meas)	$\eta\rho_m\times10^3$ (NBS standard)
NBS oil D	25.9	192.8	32.60	0.7736	18.45	18.53

In Eqs. (27) and (28), W^ν is the energy of the vibrating crystal, $W_{\text{fluid}}{}^d$ the energy dissipated when the crystal is in contact with the liquid, and $W_0{}^\nu$ the energy of the vibrating crystal in vacuum. All energies are expressed in units per cycle. The value of Q was determined from the width of the resonance curve, a typical one of which is shown in Fig. 5.

To test the absolute precision of our measurements, the viscosities of a Bureau of Standards calibrated oil and of liquid benzene were determined. It was found that the viscosities computed from Eq. (26) were in error by 4% and 9%, respectively. After careful analysis, it was decided that the discrepancy arose from a small amount of longitudinal loading. We believe this longitudinal loading to arise from a slightly misorientation of the x axis of the crystal. The increased power loss due to longitudinal loading depends on the density and the velocity of sound in a complicated way. An empirical correction can be obtained by noting that the loss is proportional to the density of the liquid. We therefore rewrite (28) in the form

$$\begin{aligned}\Delta=W^d/2W^\nu&=(W_{\text{fluid}}{}^d+W_0{}^d+\alpha\rho_m)/2W^\nu\\&=(W_{\text{fluid}}{}^d/2W^\nu)+\Delta_0+\beta\rho_m,\\ \Delta-\Delta_0-\beta\rho_m&=(\mathcal{S}/M)(\pi\eta\rho_m/\nu_0)^{\frac{1}{2}},\\ \eta\rho_m&=K'\nu[R-R_0-\gamma\rho_m]^2,\end{aligned} \tag{29}$$

with α, β, γ constants (neglecting variation of the velocity of sound). We need only determine the constant γ and then, using this correction, test our measurements against an absolute viscosity standard. From the benzene data displayed in Table III we find $\gamma=(5.05\pm0.05)\times10^3$ Ω cm^3 g^{-1} and $K'=(1.60\pm0.03)\times10^{-17}$ g^2 cm^{-4} Ω^{-2}. Using these values, the agreement between our measurements and the standard NBS oil (NBS oil D) are shown in Table IV. It is seen that the measurements agree with the NBS standardization to about 0.4%. As a further check, the viscosity of gaseous Ar was measured at 298°K at pressures ranging from 100 to 500 atm. Because of the much smaller viscosity of the gas, the precision of these measurements was lower than that of the measurements on the liquids. The agreement between our data and that of Michels[23] is within 3% everywhere in the pressure range cited.

Using the longitudinal loading correction described above, we have recorded in Table V preliminary smoothed values of the viscosity of liquid Ar at 101.8°K and 128.2°K for the range of pressures 50 to 500 atm. Further experimental measurements will be reported

TABLE V. Preliminary smoothed values of the shear viscosity of liquid Ar at 101.8°K and 128.2°K.

p (atm)	$T=128.2$°K	$T=101.8$°K
50	0.835[a]	1.667
100	0.931	1.796
150	1.029	1.921
200	1.125	2.050
250	1.220	2.180
300	1.315	2.308
350	1.410	2.435
400	1.508	2.562
450	1.602	2.690
500	1.698	2.820

[a] All viscosities are in units of millipoise. The estimated accuracy of these figures is ±2%.

in due course. The figures tabulated in Table V are estimated to be accurate to ±2%. In Fig. 6 are displayed the 101.8°K data, together with the older measurements of Scott and Zhdanova. It can be seen that the data sets differ considerably at the high-pressure end of the range.

V. DISCUSSION

It is now pertinent to test the theory developed in Secs. II and III against the available data. An examination of Fig. 6 shows that the data of Zhdanova[17] agree better with that obtained herein than do the data of Scott.[18] Indeed, the agreement is quite good. At 128°K, both the data of Zhdanova and Scott disagree with that obtained in our experiments in that the pressure dependence of the viscosity is smaller than we observe. If we accept the measurements reported herein, the computed and observed viscosities are in good agreement at 128°K and 50 atm (see Table VI). On the other hand, at 90°K and 1.3 atm there remains a discrepancy between theory and experiment of about 35%.

To examine the temperature dependence of the viscosity, we assume that the data of Zhdanova give the correct slope at constant density, even though the

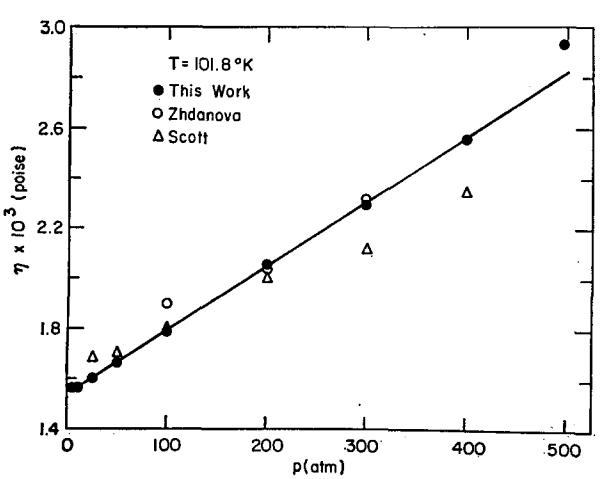

FIG. 6. The shear viscosity of liquid Ar at 101.8°K.

TABLE VI. Comparison of theoretical and observed shear viscosities.

T(°K)	p (atm)	η(calc)$\times10^3$ P	η(obs)$\times10^3$ P
128	50	0.727	0.835
90	1.3	1.74	2.39

absolute value may be in error (at 128°K and 50 atm Zhdanova reports $\eta=1.02\times10^{-3}$ P whereas we find $\eta=0.835\times10^{-3}$ P). The results of this comparison are displayed in Table VII. In view of the sensitivity of the theory to the imperfectly known radial distribution function, we consider the agreement between theory and experiment to be quite good. The theory correctly predicts that at constant density the shear viscosity is little effected by changes in temperature, the sign of the small temperature change is computed correctly, but the computed slope is larger than the observed slope if the Kirkwood value of $g^{(2)}(\sigma)$ is used.[29] Given the uncertainty of the experimental data, it is likely that the difference between the computed and experimental temperature derivatives of the shear viscosity is not significant.

A question which must be discussed after examination of our arguments is the following: Is the agreement (or disagreement) between theory and experiment significant? This question is very difficult to answer. At present, the available radial distribution functions and potential functions for a dense fluid are extremely poor. We have already noted that at liquid densities it is not uncommon to have the predicted pressure be negative. Moreover the pressure is so sensitive to the relative positions of the minimum of $u(R)$ and the first maximum of $g_0^{(2)}(R)$ that a $2\frac{1}{2}$% relative shift can change the predicted pressure from -1000 atm to $+1$ atm. From Table I we see that the equilibrium theory is worst at high densities and low temperatures (C furthest from unity). Since ψ_2 depends on $g^{(2)}$ through Eq. (16) and $\eta_V(R>\sigma)$ depends in turn on both ψ_2 and $g^{(2)}$, it is to be expected that the predicted values of η at low temperatures and high densities will be furthest from experimental values. It is our opinion that the major contribution to the observed disagree-

TABLE VII. Comparison of theoretical and observed temperature dependence of the shear viscosity at constant density, $\rho_m=1.12$ g cm^{-3}.

	128°K 50 atm	133.5°K 100 atm	185.5°K 500 atm
$\eta(\text{obs})_T/\eta(\text{obs})_{128°}$	1.00	1.01	1.04
$\eta(\text{calc})_T/\eta(\text{calc})_{128°}$	1.00	1.005	1.06 1.08[a]

[a] $g^{(2)}(\sigma)=1$.

[29] If we assume that $g^{(2)}(\sigma)=1$ at $T=185.5$°K and $p=500$ atm, then the computed and observed slopes are in quantitative agreement.

ment arises from the inadequacy of the available radial distribution function. In the program of research of which this work forms a part, excellent agreement between theory and experiment has been obtained for the cases of thermal conductivity,[14] ion mobility,[13] and self-diffusion.[30] In general, we believe the agreement between theory and experiment to be meaningful because all the calculations have been performed independently. It would be strange if the errors in $g^{(2)}(R)$ and $u(R)$ were such as to allow a large number of independent calculations to all be spuriously in good agreement with experiment. This is, however, not a very strong argument.

It is clear that complete and definitive testing of the Rice–Allnatt theory awaits the determination of very accurate equilibrium distribution functions and potential functions. The presently available agreement between theory and observation suggests (but does not prove) that the Rice–Allnatt theory is a good first order theory of transport in liquids.

[30] J. Naghizadeh and S. A. Rice, J. Chem. Phys. **36**, 2710 (1962).

ACKNOWLEDGMENTS

We wish to thank the Directorate of Chemical Sciences of the AFOSR, the Petroleum Research Fund of the American Chemical Society, and the Alfred P. Sloan Foundation for financial support. We have also benefited from the use of facilities provided by the U.S. Atomic Energy Commission and ARPA for materials research and by the NSF for low-temperature research at the University of Chicago. One of us (P.G.) has benefited from the award of a Fulbright Travel Grant by the U. S. Educational Commission.

THE JOURNAL OF CHEMICAL PHYSICS VOLUME 40, NUMBER 12 15 JUNE 1964

Gaseous Ion Recombination Rates. III

TERRY S. CARLTON* AND BRUCE H. MAHAN†

Department of Chemistry and Lawrence Radiation Laboratory,‡ University of California, Berkeley, California

(Received 21 January 1964)

The rate constants for the bimolecular recombination of gaseous ions in three different systems have been determined. The results suggest that the recombination rate constant is not particularly sensitive to the chemical identity of the ions, and that complexes between ions and neutral atoms are important even at pressures below 10 mm Hg.

IN an earlier publication, Mahan and Person[1] presented evidence that the mechanism of the mutual neutralization of gaseous ions involves two parallel processes. One of these is a bimolecular electron transfer reaction:

$$A^+ + B^- \xrightarrow{k_0} \text{neutrals}.$$

The other is essentially Thomson's[2] three-body ion recombination reaction:

$$A^+ + B^- \xrightarrow{k_1} (A^+B^-)^*,$$

$$(A^+B^-)^* \xrightarrow{k_2} A^+ + B^-,$$

$$(A^+B^-)^* + M \xrightarrow{k_3} (A^+B^-) + M \rightarrow \text{neutrals}.$$

Here $(A^+B^-)^*$ represents a pair of unbound ions closed enough to each other so that a collision of either of them with a neutral molecule M leads to formation of a bound ion pair (A^+B^-) and eventual charge neutralization. If we make the usual definition of the ion recombination coefficient α by the equation

$$-d(A^+)/dt = \alpha(A^+)(B^-),$$

then the steady-state approximation for $(A^+B^-)^*$ gives

$$\alpha = k_0 + [k_1 k_3(M)]/[k_2 + k_3(M)]. \quad (1)$$

The decision[1] that a bimolecular neutralization process exists was based on the fact that for the ions NO^+, NO_2^-, an extrapolation to zero pressure of a plot of α as a function of the pressure of M gave a finite intercept whose value was independent of the nature of M, within experimental error. We would expect that the magnitude of k_0 should depend on the nature of the recombining ions, and it is of interest to investigate this dependence. In this paper we present measurements of k_0 for three different ion systems, and a more precise evaluation of the possible dependence of k_0 on the nature of the inert gas.

* Present address: Department of Chemistry, Oberlin College, Oberlin, Ohio.
† Alfred P. Sloan Fellow.
‡ Inorganic Materials Research Division.
[1] B. H. Mahan and J. C. Person, J. Chem. Phys. **40**, 392 (1964).
[2] J. J. Thomson, Phil. Mag. **47**, 337 (1924).